iScience

Article

LINC01871 is exclusively expressed in T and NK cells and is highly induced upon CD4⁺ T cell activation

Graphical abstract

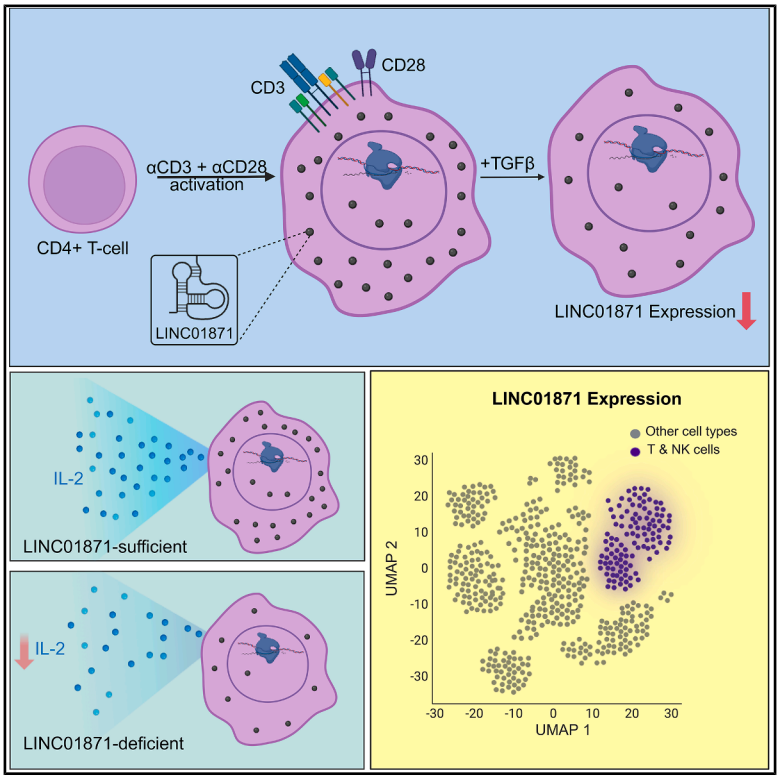

Authors

Ubaid Ullah Kalim, Ankitha Shetty, Amogh Ranade, ..., Laura L. Elo, Sanjeev Galande, Riitta Lahesmaa

Correspondence

ubaull@utu.fi (U.U.K.), rilahes@utu.fi (R.L.)

In brief

Immunology; Molecular biology; Cell biology

Highlights

- LINC01871 is a cytoplasmic lincRNA induced upon CD4⁺ T cell activation
- TGF-β negatively regulates LINC01871 expression
- Expression of LINC01871 is restricted to effector and memory T and NK cells

Kalim et al., 2025, iScience *28*, 113779
November 21, 2025
https://doi.org/10.1016/j.isci.2025.113779

CellPress

iScience

CellPress
OPEN ACCESS

Article

LINC01871 is exclusively expressed in T and NK cells and is highly induced upon CD4$^+$ T cell activation

Ubaid Ullah Kalim,[1,2,7,*] Ankitha Shetty,[1,2,6,7] Amogh Ranade,[1,2,3] Olof Rundquist,[1,2] Inna Starskaia,[1,2,3] Kedar Batkulwar,[1,2] Tommi Välikangas,[1,2] António G.G. Sousa,[1,2] Antti Hurme,[1] Venla Kumpulainen,[1] Miro Viitala,[1] Sakari Kosola,[1] Sini Junttila,[1,2] Omid Rasool,[8,1,2] Laura L. Elo,[1,2,4] Sanjeev Galande,[5] and Riitta Lahesmaa[1,2,4,8,*]

[1]Turku Bioscience Centre, University of Turku and Åbo Akademi University, Turku, Finland
[2]InFLAMES Research Flagship Center, University of Turku, Turku, Finland
[3]Turku Doctoral Programme of Molecular Medicine, University of Turku, Turku, Finland
[4]Institute of Biomedicine, University of Turku, Turku, Finland
[5]Centre of Excellence in Epigenetics, Department of Life Sciences, Shiv Nadar Institution of Eminence, Gautam Buddha Nagar, Uttar Pradesh 201314, India
[6]Present address: Department of Microbiology and Immunology, University of California San Francisco, San Francisco, CA 94143, USA
[7]These authors contributed equally
[8]Lead contact
*Correspondence: ubaull@utu.fi (U.U.K.), rilahes@utu.fi (R.L.)
https://doi.org/10.1016/j.isci.2025.113779

SUMMARY

Long intergenic noncoding RNAs (lincRNAs) regulate biological processes in health and disease. Recent findings highlight the importance of lincRNAs in regulating T cell development and function. Here, we identified a lincRNA, LINC01871, which is highly induced upon CD4$^+$ T cell activation and is predominantly located in the cytoplasm. The anti-inflammatory cytokine TGF-β was found to suppress its expression. Silencing LINC01871 led to a modest decrease in IL-2 secretion. Notably, LINC01871 expression was highly specific to NK cells and T cells in several cross-tissue single cell RNA-seq atlases. These data suggest that LINC01871 is specifically expressed in T and NK cells and may contribute to T cell-mediated immunity in humans.

INTRODUCTION

The immune system is a finely orchestrated network of molecular players that work together to maintain health and respond to threats. Among these players, long intergenic noncoding RNAs (lincRNAs) have emerged as intriguing regulators of biological processes, with a wide range of functions in both physiological and pathological context.[1] LincRNAs have been found to influence gene expression,[2] contributing to the complexity and versatility of the immune response.

High-throughput studies have identified hundreds of long noncoding RNAs (lncRNAs) to be differentially expressed (DE) during T cell activation and differentiation, with emerging evidence supporting key roles for lincRNAs in T cell development and function. For instance, the Th1-specific lincRNA Linc-MAF4 in humans has been shown to restrict Th2 differentiation by negatively regulating MAF, a Th2-specific transcription factor (TF).[3] Similarly, lincRNA Tmevpg1 was found to be upregulated in Th1 cells, coinciding with increased IFNγ expression.[4] The antisense RNA GATA3-AS1 alters the chromatin landscape of GATA3, modulating its expression along with the Th2 effector cytokines IL-5 and IL-13.[5] Additionally, lncRNAs such as H19, NEAT1, and MEG3, have been implicated in the regulation of Th17 cell differentiation.[6–8] We identified myocardial infarction-associated transcript (MIAT) as a positive regulator of Th17 cell differentiation.[9] Further, we recently reported on the role of a novel lncRNA, LIRIL2R, as a promoter of regulatory T cell function by regulating the expression of IL2RA, FOXP3, and other regulatory T cell-related genes.[10] In mice, lncRNAs Flicr and Flatr have been demonstrated to regulate Treg cell differentiation.[11,12]

In this study, we investigated a lincRNA, LINC01871 (also known as AC092580.4 in hg19:GRCh37 version of the genome), which was profoundly induced upon the activation of human CD4$^+$ T cells. We confirmed the boundaries of the transcript using rapid amplification of cDNA ends (RACE-PCR) followed by Sanger sequencing. We assessed the localization of the transcript within T cells and characterized its function during T cell activation using locked nucleic acid modified antisense oligonucleotide (LNA)-mediated silencing of the transcript. We further studied its expression in nine published single cell RNA-seq datasets to characterize cell type specificity of LINC01871.

RESULTS

LINC01871 is a cytoplasmic lincRNA highly induced upon T cell activation

Although LINC01871 was not detectable in unactivated CD4$^+$ T cells, the gene was highly induced upon activation

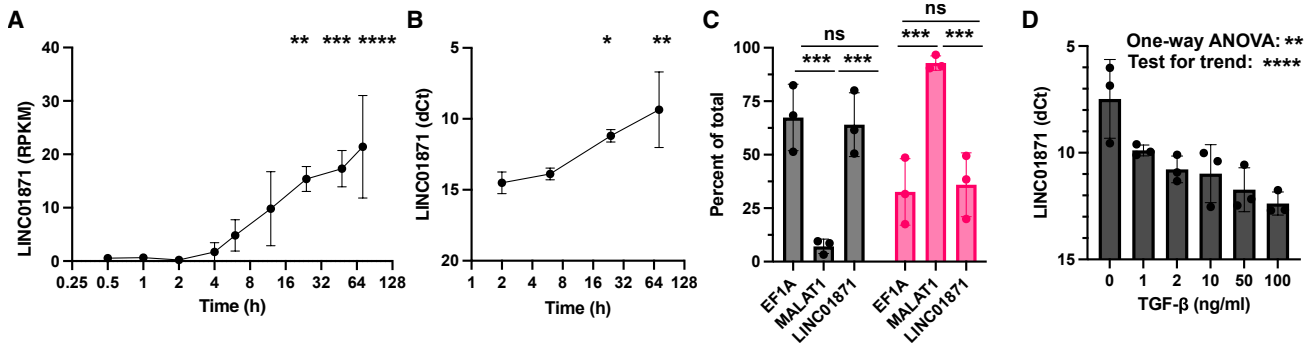

Figure 1. LINC01871 expression upon T cell activation

(A) Expression of LINC01871 upon T cell activation at different time points. The RNA-seq data were acquired from Tuomela et al.[13]

(B) LINC01871 expression was measured by TaqMan assay at different time points after activation. The EF-1α transcript was used as an internal control for calculating delta CT (dCt).

(C) Cellular location of LINC01871 in CD4$^+$ T cells activated for 72 h. EF-1α and MALAT-1 were used as cytoplasmic and nuclear RNA controls, respectively. The gray and magenta colors represent cytoplasm and nuclear fractions, respectively. Each dot represents a biological replicate where the cells were pooled from multiple (3–5) donors.

(D) LINC01871 expression when CD4$^+$ T cells were activated through TCR for 72 h in the absence (0) or presence of increasing TGF-β concentration shown on the *x* axis. For A and B, mean and standard deviation (SD) from three biological replicates have been plotted. For C and D, each dot represents an individual replicate, and error bars show the SD. The significance was determined using ordinary one-way ANOVA. For A and B, ANOVA was followed by Šídák's multiple comparisons test comparing each time point to unactivated cells. For C, ANOVA was followed by comparing selected samples of interest shown on the graph using Šídák's multiple comparisons test. For D, ANOVA was followed by test for linear trend analysis. *: $p < 0.05$, **: $p < 0.01$, ***: $p < 0.001$ ****: $p < 0.000$, ns: not significant. See also Figures S2 and S3.

of CD4$^+$ T cells in our earlier RNA-seq time-series data[13] (Figure 1A). We confirmed the TCR-induced expression of the transcript using TaqMan RT-qPCR analysis (Figure 1B), where the expression was at least 10-fold greater at 72 h of activation than in unactivated cells. To test whether the concentrations of α-CD3 and α-CD28 antibodies used in this study were optimal, we isolated naive CD4$^+$ T cells from umbilical cord blood (Figures S2A and S2B) and activated them with varying concentrations of α-CD3 and α-CD28. We observed that the concentration used in this study (3.75 μg/mL anti-CD3 and 1 μg/mL anti-CD28) was optimal: decreasing the concentration led to a reduction in the expression of T cell activation markers CD69 and IL2RA, while increasing the strength did not increase the expression of the marker genes (Figures S2C–S2E). These data indicate that the concentrations used in this study were appropriate.

LincRNAs reside in different cellular locations, e.g., nucleus[14] and cytoplasm.[15] Using cellular fractionation analysis, we found that LINC01871 is primarily localized in the cytoplasm (Figure 1C), suggestive of its role in cellular signaling. Interestingly, LINC01871 was downregulated in response to TGF-β, in a dose-dependent manner (Figure 1D). Since TGF-β dampens T cell activation,[16] we tested if its effect on LINC01871 is due to general reduction in T cell activation. We treated the cells with increasing concentration of TGF-β, and measured the lincRNA expression and the expression of T cell activation markers CD69 and IL2RA. We found that LINC01871 was downregulated upon TGF-β treatment whereas there was no significant effect on IL2RA or CD69 expression (Figure S3), confirming that TGF-β specifically acts to downregulate LINC01871 expression.

Rapid amplification of cDNA ends -PCR confirmed the expression of the LINC01871 transcript identified by RNA-seq

In the RNA-seq datasets, the transcript contained two exons, and the junction between the exons was supported by many reads.[13,17] According to Ensembl (GRCh38.p13) and LNCipedia (version 52), LINC01871 has no protein-coding potential. Further, LINC01871 appears to be encoded explicitly in humans as no homologues have been found in any other species (LNCipedia). To determine the 5′ and 3′sequence ends of the transcript, we performed rapid amplification of cDNA ends (RACE)-PCR analysis. Interestingly, in addition to the sequence of the GenBank transcript (NR_183384.1; hg38: chr2:7,725,779-7,730,721), the RACE-PCR analysis found an additional 22 nucleotides at the 5′ end (AGAC CTCCCTGCTGTGTATGTC), whereas the 3′ end was exactly as NR_183384.1, followed by poly(A) sequence (Figure S4).

LINC01871 silencing modestly reduces IL-2 secretion

To test the function of LINC01871, we silenced its expression using two different LNAs targeting the transcript (Figure S5A). LINC01871 was significantly knocked down with both LNAs (Figure 2A). The effect of the two LNAs targeting LINC01871 on cell viability and cell proliferation was similar to that of non-targeting control LNA (Figures 2B and S5B). Next, we tested the effects of LINC01871 silencing on IL-2, a cytokine secreted by activated T cells. LNA-treated cells were activated and cultured for 48 h. We observed a modest reduction in IL-2 secretion in the culture supernatants of cells treated with LNAs targeting LINC01871 as compared to those treated with control LNA (Figure 2C; Table S2). However, *IL2* mRNA showed no consistent changes (Figure 2D), suggesting that the lincRNA may post-transcriptionally regulate IL-2 levels.

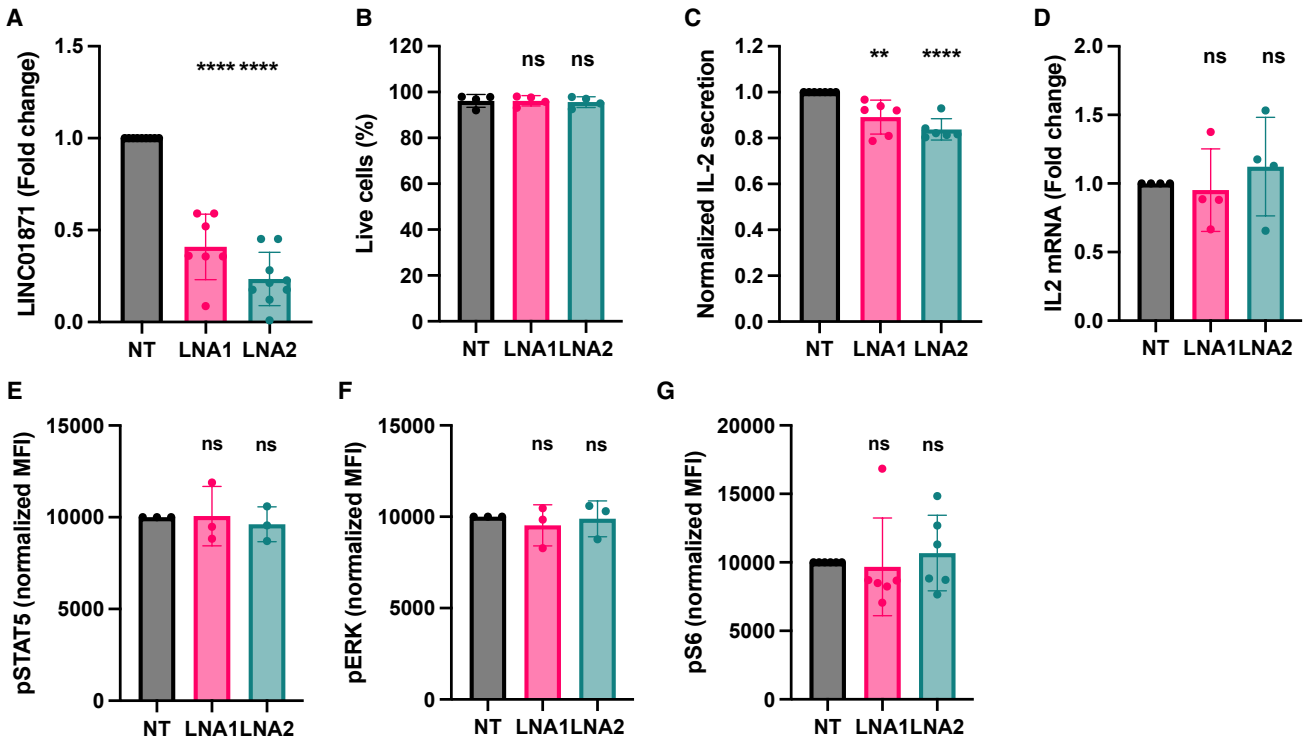

Figure 2. Effect of LINC01871 silencing on T cell activation

(A) Knockdown efficiency of LINC01871 using two different LNAs.

(B) Bar chart showing viability of cells after LNA treatment.

(C and D) Effect of LINC01871 silencing on IL-2 secretion (C) and mRNA expression (D) at 48 h time point.

(E–G) Mean fluorescence intensity (MFI) of pSTAT5 (E), pERK (F), pS6 (G) in NT, LNA1, LNA2 treated cells. In A–G, each dot is a biological replicate of cells pooled from 3 to 5 donors, and error bars show the SD. LNA1 and LNA2 treated samples have been compared with NT LNA treated samples. The significance was determined using unpaired two-tailed *t* test: **: $p < 0.01$, ****: $p < 0.0001$, ns: not significant. See also Figures S5 and S6.

We also tested the effect of LINC01871 silencing on the key phosphorylation events occurring during T cell activation using mass cytometry. We did not observe any difference in the basal or activation-induced phosphorylation of PLCγ, ZAP70, AKT, SLP76, and LCK (Figures S6A–S6E). However, we observed a small effect on the phosphorylation of ERK, STAT5, and S6 (Figures S6F–S6H), which was not consistent in the subsequent set of experiments (Figures 2E–2G).

LINC01871 silencing had a small effect on the transcriptome and proteome of T cells

To identify global targets of LINC01871, we studied the transcriptome and the proteome of LINC01871-deficient T cells, which were activated for 48 h, harvested and reactivated for 30 min followed by RNA-seq and mass spectrometry (MS) analyses (Figure S7A). Although overall correlation of expression between the two LNAs in both dataset was good (Figures S7B and S7C), the effect of LINC01871 silencing on the transcriptome and the proteome was minimal. In RNA-seq data, none of the genes were DE (FDR<0.05, LogFC>1) by both LNAs while in the MS data, five proteins were DE, all upregulated, by both LNAs: GPRIN3; ATP10A; PSMG4; FAM98C; MFSD14A (Tables S3 and S4). None of these proteins have any known function in T cell activation.

LINC01871 expression is largely restricted to T and NK cell populations

To study the expression of the LINC01871 across human tissues and cell types, we analyzed nine single cell RNA sequencing (scRNA-seq) datasets from a variety of tissues. We first focused on a large multi-organ single cell atlas from the Tabula Sapiens consortium.[18] Visualization of LINC01871 expression across cell types of Tabula Sapiens dataset demonstrated that its expression is restricted to T and NK cell populations (Figure 3A).

To validate the cell type expression, the survey was extended to eight additional immune-cell focused scRNA-seq datasets,[19–25] which confirmed that LINC01871 is consistently expressed in NK cells, MAIT cells, $CD8^+$ T cells, $CD4^+$ T cells, and innate lymphoid cells (ILCs). Among $CD4^+$ and $CD8^+$ T cells, the expression was the highest in effector T cells followed by memory cells while in naive T cells, it was very low or absent (Figure 3B), consistent with no expression in unactivated $CD4^+$ T cells isolated from cord blood (Figure 1A). Notably, expression of LINC01871 was not detected outside of the immune cell compartment in any of the studies.

To determine the functional relevance of LINC01871 expression in $CD4^+$ and $CD8^+$ T cells, we performed cell type marker analysis and identified that LINC01871 is a positive marker for effector $CD4^+$ and $CD8^+$ T cells, ILCs and MAIT cells

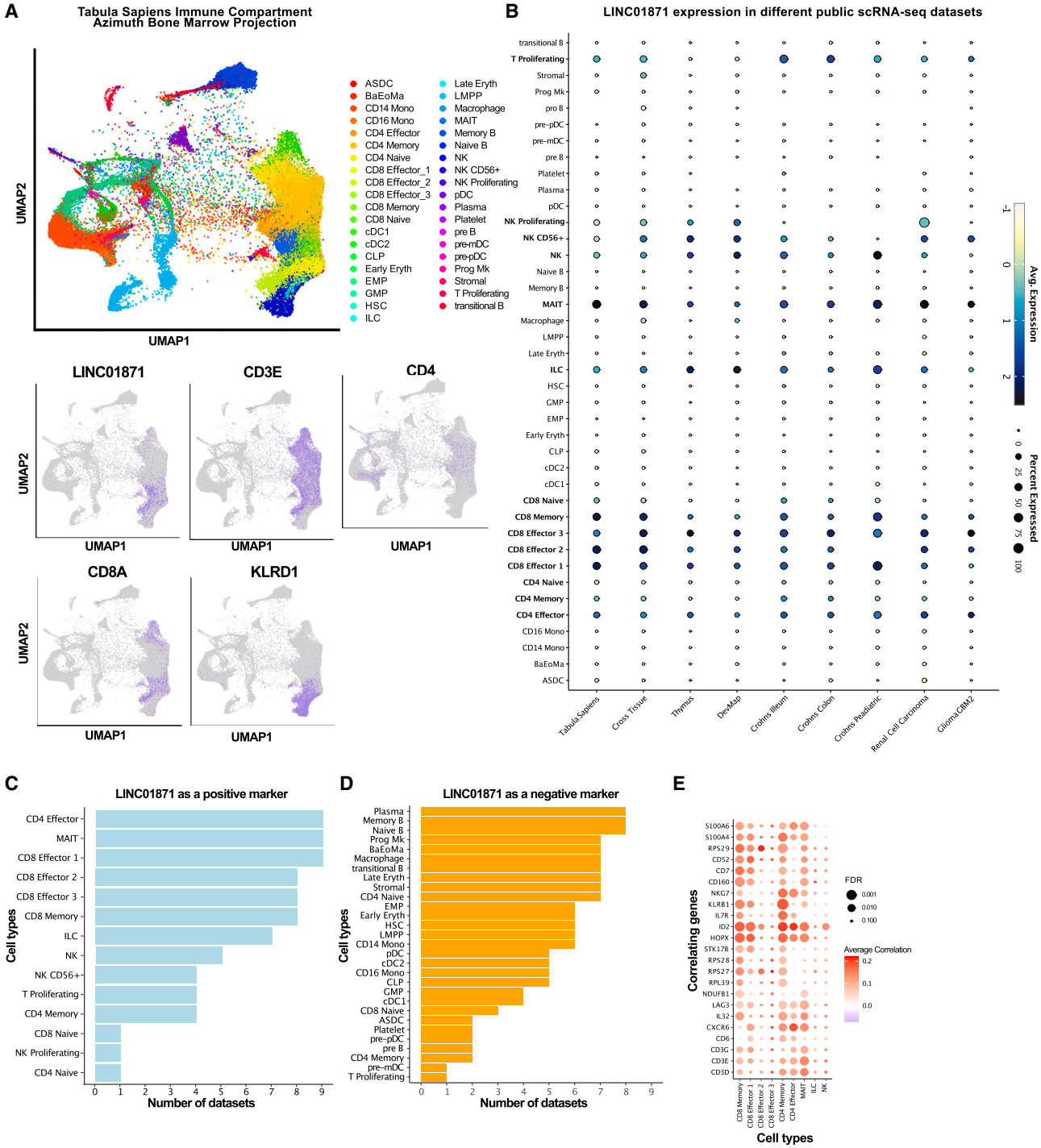

Figure 3. LINC01871 expression in Tabula sapiens and cross tissue immune datasets

(A) UMAPs of cell type clusters in the Tabula sapiens immune compartment. The upper panel shows clusters of different cell types and the lower panels show the expression of LINC01871 along with the markers of T and NK cells.

(B) Dot plots showing the expression of LINC01871 in given cell type clusters in the respective datasets.

(C and D) Show the number of datasets among 9 selected scRNA-seq data where LINC01871 was positive or negative marker for given cell types, respectively.

(E) Cell type-specific LINC01871-co-expressing genes from all datasets. Mean gene correlation for top genes to LINC01871 expression in cell types have been visualized. Only cell types showing consistent LINC01871 expression were evaluated. Correlations were considered significant if different from 0 (*t* test) and greater than 0.2 or less than −0.2. The cell type annotation was performed by reference with Azimuth, using the bone marrow (BM) reference. The expression in the dot plots has been scaled against the number of cells.

in multiple datasets and a negative marker for non-T cells, particularly plasma cells and B cells (Figures 3C and 3D).

Finally, we assayed which genes were correlated with LINC01871 in each cell type. Many genes with effector T cell and NK cell function, such as KLRB1, IL32, and CD160, had positive correlation with LINC01871 in different $CD4^+$ and $CD8^+$ effector and memory T cells (Figure 3E).

DISCUSSION

A key discovery of our study is the unique expression pattern of LINC01871, which appears to be almost exclusively expressed in T and NK cell populations. Our findings indicate that LINC01871 is a cytoplasmic lincRNA, markedly upregulated upon T cell activation, and possibly involved in post-transcriptional regulation of IL-2 secretion. The observed downregulation of LINC01871 in response to TGF-β suggests its involvement in immune response modulation, given TGF-β's well-established role in immune regulation and T cell differentiation.[26,27]

The cytoplasmic localization of LINC01871 suggests a role in regulating cytoplasmic processes, such as acting as a microRNA sponge. Indeed, LINC01871 has previously been reported to act as sponge for miR-142–3p leading to overexpression of the miRNA target ZYG11B, which in turn promoted the chemoresistance of colorectal cancer cells via autophagy induction.[28] Interestingly, LINC01871 has been included in the lncRNA signatures predictive of melanoma,[29] adenocarcinoma,[30] endometrial,[31,32] and cervical cancer.[33,34] Further studies are needed to investigate if the expression of LINC10871 in cancer tissues is derived from cancer cells, associated stroma, tumor infiltrating lymphocytes, or other immune cells.

Several earlier studies have identified LINC01871 as a part of autophagy related lncRNA signature for prognosis of breast cancer.[35–38] Another function to which LINC01871 has been associated is the various forms of cell death pathways including necrosis,[30] necroptosis,[39–41] and ferroptosis.[42,43] However, our data did not show any impact on genes/proteins involved in these pathways.

Upregulation of LINC01871 upon T cell activation and its positive impact on IL-2 secretion, together with the results showing LINC01871 downregulation by the anti-inflammatory cytokine TGF-β, may suggest that the lincRNA is a proinflammatory factor. This role is further supported by its upregulation in $CD4^+$ T cells from prediabetic children progressing to islet autoimmunity.[44] Interestingly, LINC01871 was coregulated with proinflammatory cytokine IL32 in multiple single cell RNA-seq datasets (Figure 3E) and in our earlier report, where LINC01871 and IL32 were part of coregulated gene expression clusters associated with type 1 diabetes autoimmunity.[44]

Limitations of the study

A limitation of the study is that we did not observe a strong effect of LINC01871 silencing on the gene expression at RNA or protein levels suggesting that the lincRNA may have function beyond gene expression, especially given the cytoplasmic localization of this lincRNA. For instance, it could sequester proteins or RNAs from binding to other targets or could affect posttranslational modification of proteins by interacting with kinases/phosphatases as was shown for a STAT3-interacting cytoplasmic lncRNA.[15] Another concern was a poor overlap of the two LNAs for their effect on the target genes, which could be due to their differential silencing efficiency. Furthermore, the effect of LINC01871 silencing on IL-2 secretion was rather weak. Cord blood was obtained as anonymized samples, and information on sex and gender of donors was not available to the researchers. Findings should thus be interpreted with caution regarding their generalizability across sexes.

RESOURCE AVAILABILITY

Lead contact

Further information and requests for resources should be directed to the lead contact, Riitta Lahesmaa (rilahes@utu.fi).

Materials availability

This study did not generate new reagents.

Data and code availability

- Raw and processed RNA-seq data have been submitted to NCBI GEO database and are publicly available with accession number GEO: GSE268455. The MS raw and peaks files of the whole-cell proteome have been deposited to ProteomeXchange via PRIDE,[45] and are publicly available with project accession ID PRIDE: PXD052298. Differentially expressed genes and proteins in this study have been deposited as Mendeley data and are publicly available (Mendeley Data: https://doi.org/10.17632/ff2p5s5dzn.1).
- This study did not generate any original/custom code.
- Any additional information required to reanalyze the data reported in this paper is available from the lead contact upon request.

ACKNOWLEDGMENTS

We acknowledge the core facilities at Turku Bioscience Center: The Finnish Functional Genomics Center, Cell Imaging and Cytometry Core, and Proteomics Facility, supported by Biocenter Finland, for their assistance in next-generation sequencing, flow cytometry and imaging, and mass spectrometry analyses, respectively. The Finnish Center for Scientific Computing is duly acknowledged for its efficient servers and data analysis resources. R.L. is supported by Research Council of Finland grants 250114, 292335, 294337, 292482, 319280, 329277, 331793, 335435, and 31444; Breakthrough T1D Foundation grant; the Novo Nordisk Foundation grant NNF19OC0057218; Jane and Aatos Erkko Foundation grant; and the Finnish Cancer Foundation grant. L.L.E. is supported by European Research Council ERC 677943, European Union's Horizon 2020 research and innovation program 955321; and Research Council of Finland grants 310561, 314443, 329278, 335434, 335611, and 341342. R.L. and L.L.E. were supported by the Sigrid Jusélius Foundation, Turku Graduate School University of Turku, Åbo Akademi University InFLAMES Flagship Program of the Research Council of Finland 337530, Biocenter Finland, and ELIXIR Finland. AGGS was supported by the European Union's Horizon 2020 Research and Innovation Program under the Marie Skłodowska-Curie grant agreement no.: 955321. O Rundquist. was supported by the Finnish Cultural Foundation and the Sakari Alhopuro Foundation grants, K.B. was supported by the Finnish Cultural Foundation grant.

AUTHOR CONTRIBUTIONS

U.U.K., A.S., A.R., O Rasool, and R.L. designed the study; U.U.K., A.S., A.R., I.S., K.B., T.V., A.H., V.K., M.V., S.K., O Rasool, and R.L. performed research; U.U.K., A.S., A.R., O Rundquist, I.S., K.B., T.V., S.J., A.G.G.S., A.H., V.K., M.V., S.K., O Rasool, analyzed data; U.U.K., O Rasool, S.J., L.L.E., and R.L. supervised the study. U.U.K., A.S., A.R., O Rundquist, O Rasool, L.L.E., and R.L. wrote the paper. All authors revised and approved the manuscript.

DECLARATION OF INTERESTS

The authors declare no conflict of interests.

DECLARATION OF GENERATIVE AI AND AI-ASSISTED TECHNOLOGIES IN THE WRITING PROCESS

During the preparation of this work the author(s) used ChatGPT in order to improve English language. After using this tool, the author(s) reviewed and edited the content as needed and take full responsibility for the content of the publication.

STAR★METHODS

Detailed methods are provided in the online version of this paper and include the following:

- KEY RESOURCES TABLE
- EXPERIMENTAL MODEL AND STUDY PARTICIPANT DETAILS
  - Institutional review board statement
  - Human primary T cell isolation, activation, and culture conditions
  - Controls
- METHOD DETAILS
  - T cell activation titration, cell viability and proliferation assay
  - Gene knockdown
  - Cellular fractionation
  - RNA isolation and TaqMan qRT-PCR assay
  - RNA-seq analysis
  - Mass spectrometry (MS)
  - Mass cytometry
  - ELISA
  - RACE-PCR and sanger sequencing
  - Reanalysis of published scRNA-seq datasets
- QUANTIFICATION AND STATISTICAL ANALYSIS

SUPPLEMENTAL INFORMATION

Supplemental information can be found online at https://doi.org/10.1016/j.isci.2025.113779.

Received: October 7, 2024
Revised: May 5, 2025
Accepted: October 13, 2025
Published: October 15, 2025

REFERENCES

1. Mattick, J.S., Amaral, P.P., Carninci, P., Carpenter, S., Chang, H.Y., Chen, L.L., Chen, R., Dean, C., Dinger, M.E., Fitzgerald, K.A., et al. (2023). Long non-coding RNAs: definitions, functions, challenges and recommendations. Nat. Rev. Mol. Cell Biol. *24*, 430–447. https://doi.org/10.1038/s41580-022-00566-8.
2. Statello, L., Guo, C.J., Chen, L.L., and Huarte, M. (2021). Gene regulation by long non-coding RNAs and its biological functions. Nat. Rev. Mol. Cell Biol. *22*, 96–118. https://doi.org/10.1038/s41580-020-00315-9.
3. Ranzani, V., Rossetti, G., Panzeri, I., Arrigoni, A., Bonnal, R.J., Curti, S., Gruarin, P., Provasi, E., Sugliano, E., Marconi, M., et al. (2015). The long intergenic noncoding RNA landscape of human lymphocytes highlights the regulation of T cell differentiation by linc-MAF-4. Nat. Immunol. *16*, 318–325. https://doi.org/10.1038/ni.3093.
4. Collier, S.P., Collins, P.L., Williams, C.L., Boothby, M.R., and Aune, T.M. (2012). Cutting edge: influence of Tmevpg1, a long intergenic noncoding RNA, on the expression of Ifng by Th1 cells. J. Immunol. *189*, 2084–2088. https://doi.org/10.4049/jimmunol.1200774.
5. Gibbons, H.R., Shaginurova, G., Kim, L.C., Chapman, N., Spurlock, C.F., and Aune, T.M. (2018). Divergent lncRNA GATA3-AS1 Regulates GATA3 Transcription in T-Helper 2 Cells. Front. Immunol. *9*, 2512. https://doi.org/10.3389/fimmu.2018.02512.
6. Liu, Z., Liu, L., Zhong, Y., Cai, M., Gao, J., Tan, C., Han, X., Guo, R., and Han, L. (2019). LncRNA H19 over-expression inhibited Th17 cell differentiation to relieve endometriosis through miR-342-3p/IER3 pathway. Cell Biosci. *9*, 84. https://doi.org/10.1186/s13578-019-0346-3.
7. Shui, X., Chen, S., Lin, J., Kong, J., Zhou, C., and Wu, J. (2019). Knockdown of lncRNA NEAT1 inhibits Th17/CD4+ T cell differentiation through reducing the STAT3 protein level. J. Cell. Physiol. *234*, 22477–22484. https://doi.org/10.1002/jcp.28811.
8. Qiu, Y.Y., Wu, Y., Lin, M.J., Bian, T., Xiao, Y.L., and Qin, C. (2019). LncRNA-MEG3 functions as a competing endogenous RNA to regulate Treg/Th17 balance in patients with asthma by targeting microRNA-17/RORγt. Biomed. Pharmacother. *111*, 386–394. https://doi.org/10.1016/j.biopha.2018.12.080.
9. Khan, M.M., Khan, M.H., Kalim, U.U., Khan, S., Junttila, S., Paulin, N., Kong, L., Rasool, O., Elo, L.L., and Lahesmaa, R. (2022). Long Intergenic Noncoding RNA MIAT as a Regulator of Human Th17 Cell Differentiation. Front. Immunol. *13*, 856762. https://doi.org/10.3389/FIMMU.2022.856762.
10. Andrabi, S.B.A., Kalim, U.U., Palani, S., Khan, M.M., Khan, M.H., Fagersund, J., Orpana, J., Paulin, N., Batkulwar, K., Junttila, S., et al. (2024). Long noncoding RNA LIRIL2R modulates FOXP3 levels and suppressive function of human CD4+ regulatory T cells by regulating IL2RA. Proc. Natl. Acad. Sci. USA *121*, e2315363121. https://doi.org/10.1073/pnas.2315363121.
11. Zemmour, D., Pratama, A., Loughhead, S.M., Mathis, D., and Benoist, C. (2017). Flicr, a long noncoding RNA, modulates Foxp3 expression and autoimmunity. Proc. Natl. Acad. Sci. USA *114*, E3472–E3480. https://doi.org/10.1073/pnas.1700946114.
12. Brajic, A., Franckaert, D., Burton, O., Bornschein, S., Calvanese, A.L., Demeyer, S., Cools, J., Dooley, J., Schlenner, S., and Liston, A. (2018). The long non-coding RNA Flatr anticipates Foxp3 expression in regulatory T cells. Front. Immunol. *9*, 1989. https://doi.org/10.3389/fimmu.2018.01989.
13. Tuomela, S., Rautio, S., Ahlfors, H., Öling, V., Salo, V., Ullah, U., Chen, Z., Hämälistö, S., Tripathi, S.K., Äijö, T., et al. (2016). Comparative analysis of human and mouse transcriptomes of Th17 cell priming. Oncotarget *7*, 13416–13428. https://doi.org/10.18632/oncotarget.7963.
14. Cabili, M.N., Dunagin, M.C., McClanahan, P.D., Biaesch, A., Padovan-Merhar, O., Regev, A., Rinn, J.L., and Raj, A. (2015). Localization and abundance analysis of human lncRNAs at single-cell and single-molecule resolution. Genome Biol. *16*, 20. https://doi.org/10.1186/s13059-015-0586-4.
15. Wang, P., Xue, Y., Han, Y., Lin, L., Wu, C., Xu, S., Jiang, Z., Xu, J., Liu, Q., and Cao, X. (2014). The STAT3-binding long noncoding RNA lnc-DC controls human dendritic cell differentiation. Science *344*, 310–313. https://doi.org/10.1126/science.1251456.
16. Chen, C.H., Seguin-Devaux, C., Burke, N.A., Oriss, T.B., Watkins, S.C., Clipstone, N., and Ray, A. (2003). Transforming growth factor β blocks Tec kinase phosphorylation, Ca2+ influx, and NFATc translocation causing inhibition of T cell differentiation. J. Exp. Med. *197*, 1689–1699. https://doi.org/10.1084/jem.20021170.
17. Ubaid, U., Andrabi, S.B.A., Tripathi, S.K., Dirasantha, O., Kanduri, K., Rautio, S., Gross, C.C., Lehtimäki, S., Bala, K., Tuomisto, J., et al. (2018). Transcriptional Repressor HIC1 Contributes to Suppressive Function of Human Induced Regulatory T Cells. Cell Rep. *22*, 2094–2106. https://doi.org/10.1016/j.celrep.2018.01.070.
18. Tabula Sapiens Consortium, Jones, R.C., Karkanias, J., Krasnow, M.A., Pisco, A.O., Quake, S.R., Salzman, J., Yosef, N., Bulthaup, B., Brown, P., et al. (2022). The Tabula Sapiens: A multiple-organ, single-cell transcriptomic atlas of humans. Science *376*, eabl4896. https://doi.org/10.1126/science.abl4896.

19. Park, J.E., Botting, R.A., Conde, C.D., Popescu, D.M., Lavaert, M., Kunz, D.J., Goh, I., Stephenson, E., Ragazzini, R., Tuck, E., et al. (2020). A cell atlas of human thymic development defines T cell repertoire formation. Science *367*, eaay3224. https://doi.org/10.1126/science.aay3224.

20. Abdelfattah, N., Kumar, P., Wang, C., Leu, J.S., Flynn, W.F., Gao, R., Baskin, D.S., Pichumani, K., Ijare, O.B., Wood, S.L., et al. (2022). Single-cell analysis of human glioma and immune cells identifies S100A4 as an immunotherapy target. Nat. Commun. *13*, 767. https://doi.org/10.1038/s41467-022-28372-y.

21. Bi, K., He, M.X., Bakouny, Z., Kanodia, A., Napolitano, S., Wu, J., Grimaldi, G., Braun, D.A., Cuoco, M.S., Mayorga, A., et al. (2021). Tumor and immune reprogramming during immunotherapy in advanced renal cell carcinoma. Cancer Cell *39*, 649–661.e5. https://doi.org/10.1016/j.ccell.2021.02.015.

22. Elmentaite, R., Ross, A.D.B., Roberts, K., James, K.R., Ortmann, D., Gomes, T., Nayak, K., Tuck, L., Pritchard, S., Bayraktar, O.A., et al. (2020). Single-Cell Sequencing of Developing Human Gut Reveals Transcriptional Links to Childhood Crohn's Disease. Dev. Cell *55*, 771–783.e5. https://doi.org/10.1016/j.devcel.2020.11.010.

23. Kong, L., Pokatayev, V., Lefkovith, A., Carter, G.T., Creasey, E.A., Krishna, C., Subramanian, S., Kochar, B., Ashenberg, O., Lau, H., et al. (2023). The landscape of immune dysregulation in Crohn's disease revealed through single-cell transcriptomic profiling in the ileum and colon. Immunity *56*, 444–458.e5. https://doi.org/10.1016/j.immuni.2023.01.002.

24. Suo, C., Dann, E., Goh, I., Jardine, L., Kleshchevnikov, V., Park, J.E., Botting, R.A., Stephenson, E., Engelbert, J., Tuong, Z.K., et al. (2022). IMMUNOLOGY Mapping the developing human immune system across organs. Science *376*, eabo0510. https://doi.org/10.1126/science.abo0510.

25. Domínguez Conde, C., Xu, C., Jarvis, L.B., Rainbow, D.B., Wells, S.B., Gomes, T., Howlett, S.K., Suchanek, O., Polanski, K., King, H.W., et al. (2022). Cross-tissue immune cell analysis reveals tissue-specific features in humans. Science *376*, eabl5197. https://doi.org/10.1126/science.abl5197.

26. Li, M.O., Wan, Y.Y., Sanjabi, S., Robertson, A.K.L., and Flavell, R.A. (2006). Transforming growth factor-β regulation of immune responses. Annu. Rev. Immunol. *24*, 99–146. https://doi.org/10.1146/annurev.immunol.24.021605.090737.

27. Chen, W. (2023). TGF-β Regulation of T Cells. Annu. Rev. Immunol. *41*, 483–512. https://doi.org/10.1146/annurev-immunol-101921-045939.

28. Duan, B., Zhang, H., Zhu, Z., Yan, X., Ji, Z., and Li, J. (2023). LncRNA LINC01871 sponging miR-142-3p to modulate ZYG11B promotes the chemoresistance of colorectal cancer cells by inducing autophagy. Anticancer. Drugs *34*, 827–836. https://doi.org/10.1097/CAD.0000000000001478.

29. Li, Z., Wei, J., Zheng, H., Zhang, Y., Song, M., Cao, H., and Jin, Y. (2022). The new horizon of biomarker in melanoma patients A study based on autophagy-related long non-coding RNA. Med. (United States) *101*, e28553. https://doi.org/10.1097/MD.0000000000028553.

30. Wu, N., Chen, J., Lin, T., Zhong, Z., Li, M., Yu, Y., Guo, J., and Yu, W. (2024). Identification of AP002498.1 and LINC01871 as prognostic biomarkers and therapeutic targets for distant metastasis of colorectal adenocarcinoma. Cancer Med. *13*, e6823. https://doi.org/10.1002/cam4.6823.

31. Wang, Z., Zhang, J., Liu, Y., Zhao, R., Zhou, X., and Wang, H. (2020). An Integrated Autophagy-Related Long Noncoding RNA Signature as a Prognostic Biomarker for Human Endometrial Cancer: A Bioinformatics-Based Approach. BioMed Res. Int. *2020*, 5717498. https://doi.org/10.1155/2020/5717498.

32. Wang, Z., Liu, Y., Zhang, J., Zhao, R., Zhou, X., and Wang, H. (2021). An Immune-Related Long Noncoding RNA Signature as a Prognostic Biomarker for Human Endometrial Cancer. J. Oncol. *2021*, 9972454. https://doi.org/10.1155/2021/9972454.

33. Chen, Q., Hu, L., Huang, D., Chen, K., Qiu, X., and Qiu, B. (2020). Six-lncRNA Immune Prognostic Signature for Cervical Cancer. Front. Genet. *11*, 533628. https://doi.org/10.3389/fgene.2020.533628.

34. Xu, M., Zhang, R., and Qiu, J. (2022). A four immune-related long noncoding RNAs signature as predictors for cervical cancer. Hum. Cell *35*, 348–359. https://doi.org/10.1007/s13577-021-00654-5.

35. Wu, Q., Li, Q., Zhu, W., Zhang, X., and Li, H. (2021). Identification of autophagy-related long non-coding RNA prognostic signature for breast cancer. J. Cell Mol. Med. *25*, 4088–4098. https://doi.org/10.1111/jcmm.16378.

36. Li, X., Jin, F., and Li, Y. (2021). A novel autophagy-related lncRNA prognostic risk model for breast cancer. J. Cell Mol. Med. *25*, 4–14. https://doi.org/10.1111/jcmm.15980.

37. Chen, J., Li, X., Yan, S., Li, J., Zhou, Y., Wu, M., Ding, J., Yang, J., Yuan, Y., Zhu, Y., and Wu, W. (2022). An autophagy-related long non-coding RNA prognostic model and related immune research for female breast cancer. Front. Oncol. *12*, 929240. https://doi.org/10.3389/fonc.2022.929240.

38. Luo, Z., Nong, B., Ma, Y., and Fang, D. (2022). Autophagy related long non-coding RNA and breast cancer prognosis analysis and prognostic risk model establishment. Ann. Transl. Med. *10*, 58. https://doi.org/10.21037/atm-21-6251.

39. Liu, J., Luo, B., Zhang, P., Jiang, K., Hou, Z., Cao, X., and Tang, J. (2023). Necroptosis-related LncRNAs in skin cutaneous melanoma: evaluating prognosis, predicting immunity, and guiding therapy. BMC Cancer *23*, 752. https://doi.org/10.1186/s12885-023-11246-x.

40. Tao, S., Tao, K., and Cai, X. (2022). Necroptosis-Associated lncRNA Prognostic Model and Clustering Analysis: Prognosis Prediction and Tumor-Infiltrating Lymphocytes in Breast Cancer. J. Oncol. *2022*, 7099930. https://doi.org/10.1155/2022/7099930.

41. Cui, Z., Liang, Z., Song, B., Zhu, Y., Chen, G., Gu, Y., Liang, B., Ma, J., and Song, B. (2023). Machine learning-based signature of necrosis-associated lncRNAs for prognostic and immunotherapy response prediction in cutaneous melanoma and tumor immune landscape characterization. Front. Endocrinol. *14*, 1180732. https://doi.org/10.3389/fendo.2023.1180732.

42. Xu, Z., Jiang, S., Ma, J., Tang, D., Yan, C., and Fang, K. (2021). Comprehensive Analysis of Ferroptosis-Related LncRNAs in Breast Cancer Patients Reveals Prognostic Value and Relationship With Tumor Immune Microenvironment. Front. Surg. *8*, 742360. https://doi.org/10.3389/fsurg.2021.742360.

43. Xu, Y., Chen, Y., Niu, Z., Yang, Z., Xing, J., Yin, X., Guo, L., Zhang, Q., Yang, Y., and Han, Y. (2022). Ferroptosis-related lncRNA signature predicts prognosis and immunotherapy efficacy in cutaneous melanoma. Front. Surg. *9*, 860806. https://doi.org/10.3389/fsurg.2022.860806.

44. Kallionpää, H., Somani, J., Tuomela, S., Ullah, U., de Albuquerque, R., Lönnberg, T., Komsi, E., Siljander, H., Honkanen, J., Härkönen, T., et al. (2019). Early Detection of Peripheral Blood Cell Signature in Children Developing β-Cell Autoimmunity at a Young Age. Diabetes *68*, 2024–2034. https://doi.org/10.2337/db19-0287.

45. Perez-Riverol, Y., Bai, J., Bandla, C., García-Seisdedos, D., Hewapathirana, S., Kamatchinathan, S., Kundu, D.J., Prakash, A., Frericks-Zipper, A., Eisenacher, M., et al. (2022). The PRIDE database resources in 2022: A hub for mass spectrometry-based proteomics evidences. Nucleic Acids Res. *50*, D543–D552. https://doi.org/10.1093/nar/gkab1038.

46. Andrews, S. (2010). FastQC: A Quality Control Tool for High Throughput Sequence Data. [Online]. Available online at: http://www.bioinformatics.babraham.ac.uk/projects/fastqc/

47. Liao, Y., Smyth, G.K., and Shi, W. (2019). The R package Rsubread is easier, faster, cheaper and better for alignment and quantification of RNA sequencing reads. Nucleic Acids Res. *47*, e47. https://doi.org/10.1093/nar/gkz114.

48. Robinson, M.D., McCarthy, D.J., and Smyth, G.K. (2010). edgeR: A Bioconductor package for differential expression analysis of digital gene expression data. Bioinformatics *26*, 139–140. https://doi.org/10.1093/bioinformatics/btp616.

49. Suomi, T., Seyednasrollah, F., Jaakkola, M.K., Faux, T., and Elo, L.L. (2017). ROTS: An R package for reproducibility-optimized statistical testing. PLoS Comput. Biol. *13*, e1005562. https://doi.org/10.1371/journal.pcbi.1005562.

50. Hao, Y., Stuart, T., Kowalski, M.H., Choudhary, S., Hoffman, P., Hartman, A., Srivastava, A., Molla, G., Madad, S., Fernandez-Granda, C., and Satija, R. (2024). Dictionary learning for integrative, multimodal and scalable single-cell analysis. Nat. Biotechnol. *42*, 293–304. https://doi.org/10.1038/s41587-023-01767-y.

51. Blanco-Carmona, E. (2022). Generating publication ready visualizations for Single Cell transcriptomics using SCpubr. Preprint at bioRxiv. https://doi.org/10.1101/2022.02.28.482303.

52. Hamalainen, H.K., Tubman, J.C., Vikman, S., Kyrölä, T., Ylikoski, E., Warrington, J. a, and Lahesmaa, R. (2001). Identification and validation of endogenous reference genes for expression profiling of T helper cell differentiation by quantitative real-time RT-PCR. Anal. Biochem. *299*, 63–70. https://doi.org/10.1006/abio.2001.5369.

53. Hailemariam, M., Eguez, R.V., Singh, H., Bekele, S., Ameni, G., Pieper, R., and Yu, Y. (2018). S-Trap, an Ultrafast Sample-Preparation Approach for Shotgun Proteomics. J. Proteome Res. *17*, 2917–2924. https://doi.org/10.1021/acs.jproteome.8b00505.

STAR★METHODS

KEY RESOURCES TABLE

REAGENT or RESOURCE	SOURCE	IDENTIFIER
Antibodies		
anti-pS6 -175Lu, [S235/S236], clone N7-548	Standard Biotools	Cat#3175009A; RRID: AB_2811251
anti-pPLCg2 – 144Nd [Y759], clone K86-689.37	Standard Biotools	Cat#3144015A; RRID: AB_3677800
anti-pERK1/2 – 167Er [T202/Y204], clone D1314.4E	Standard Biotools	Cat#3167005A; RRID: AB_2661834
anti-pSLP-76 – 156Gd [Y128], clone J141-668.36.58	Standard Biotools	Cat#3156003A; RRID: AB_2827885
anti-pZAP70 - 171Yb [Y319]/pSyk [Y352], clone 17a	Standard Biotools	Cat#3171005A; RRID: AB_2827884
anti-pLck – 162Dy [T505], clone 4/LCK-Y505	Standard Biotools	Cat#3162004A; RRID: AB_2827886
anti-pAkt – 152Sm [S473], clone D9E	Standard Biotools	Cat#3152005A; RRID: AB_2811246
anti-pStat5 – 150Nd [Y694], clone 47	Standard Biotools	Cat#3150005A; RRID: AB_2744690
anti-CD3	Beckman Coulter	Cat#IM1304; RRID: AB_131612
anti-CD28	Beckman Coulter	Cat#IM1376; RRID: AB_131624
anti-CD69	BD Pharmigen	Cat#347823; RRID: AB_400353
anti-CD25	BD Pharmigen	Cat#567316; RRID: AB_3683785
Human IL-2 DuoSet ELISA	R&D Systems	Cat#DY202-05, DY008
Chemicals, peptides, and recombinant proteins		
rhTGF-β1	R & D systems	Cat#240-B
Cell ID cisplatin	Standard Biotools	201064
Fixable Viability Dye eFluor™ 780	eBioscience™	Cat#65-0865-14
OptiMEM medium	Gibco by Life Technologies	Cat#31985-047
Protease Cocktail Inhibitor	Roche Systems	Cat#4693132001
DNase I	Invitrogen	Cat#18047019
SuperScript II Reverse Transcriptase	Invitrogen	Cat#18064-014 Cat#18418012
Critical commercial assays		
Dynal CD4 Positive Isolation Kit	Invitrogen	Cat#11331D
EasySep™ Human Naïve CD4+ T Cell Isolation Kit	Stemcell Technologies	Cat#18000
RNeasy Mini Kit	Qiagen	Cat#74104
RNAse-Free DNA set	Qiagen	Cat# 79254
Maxpar Cell acquisition solution	Standard Biotools	Cat#201244
Cell-ID Intercalator Solution	Standard Biotools	Cat#201192B
SMARTer RACE cDNA Amplification Kit	Takara Bio/Clontech	Cat#634858 Cat#634859
GeneJet Gel Extraction Kit	Thermofisher scientific	Cat#K0692
Absolute QPCR Mix, ROX	Thermofischer scientific	Cat#AB1139A
Deposited data		
Data used from another study: Cross-tissue	Domínguez Conde C, et al.[25]	
Data used from another study: Thymus	Park JE et al.[19]	
Data used from another study: DevMap	Suo C et al.[24]	
Data used from another study: Crohns Illeum	Kong L et al.[23]	

(*Continued on next page*)

Continued

REAGENT or RESOURCE	SOURCE	IDENTIFIER
Data used from another study: Crohns Colon	Kong L et al.[23]	
Data used from another study: Crohns Pediatric	Elmentaite R et al.[22]	
Data used from another study: Glioma	Abdelfattah, N. et al.[20]	
Data used from another study: RCC	Bi K et al.[21]	
Data used from another study: Tabula	Jones et al.,[18]	
Data Deposited: Mendeley Data	Mendeley database	Mendeley data: https://doi.org/10.17632/ff2p5s5dzn.1
Data deposited: RNA-seq	NCBI Geo Database	GEO: GSE268455
Data deposited: MS raw and peaks files	ProteomeXchange	PRiDE: PXD052298
Oligonucleotides		
5'-RACE primer	IDT	5'-gcatgctgaacccaggcagctgactccagag-3'
3'-RACE primer	IDT	5'-ctctggagtcagctgcctgggttcagcatgc-3'
5'-RACEnested primer	IDT	5'-ctctgttgctcagcttcggcctttgg-3
3'-RACEnested primer	IDT	5'-gctgccgtggacgatctgtctctc-3'
LNA1	IDT	5'-TTCGGCCTTTGGTAGT-3'
LNA2	IDT	5'-ACAGATCGTCCACGGC-3'
non-targeting LNA (NT)	IDT	5'-AACACGTCTATACGC-3'
LINC01871 TaqMan	Roche	forward: 5'-agcatgcagcaactacagtca-3'; reverse: 5'-cagcttcggcctttggta-3', and probe #78 from Roche Universal Probe Library (UPL)
EF1-α TaqMan	Roche	forward primer: 5'-ctgaaccatccaggccaaat-3', reverse primer: 5'-gccgtgtggcaatccaat-3',Probe FAM-TAMRA: 5'-agcgccggctatgcccctg-3'
MALAT1 TaqMan	Roche	forward primer: 5'-gacccttcacccctcacc-3', reverse primer: 5'-ttatggatcatgcccacaag-3' and probe #71 from Universal Probe Library(UPL).
CD69 TaqMan	Thermofisher Scientific	Hs00934033_m1
IL-2RA TaqMan	Roche	forward primer: 5'-acgggaagacaaggtggac-3', reverse primer: 5'-tgcctgaggcttctcttca-3', and Probe #54 from Universal Probe Library
Software and algorithms		
QuantStudio	Thermo Fisher Scientific	https://www.thermofisher.com/fi/en/home/global/forms/life-science/quantstudio-6-7-flex-software.html?erpType=Global_E1
GraphPad Prism 9.0.2	GraphPad	https://www.graphpad.com/features
FCS Express 7 Flow software v. 7	*De Novo* Software, USA	https://denovosoftware.com/full-access/download-landing/
Biorender	Biorender	https://www.biorender.com/
FastQC v.0.11.8	Andrews S. et al.[46]	https://www.bioinformatics.babraham.ac.uk/projects/fastqc/
Rsubread v.2.6.4	Liao Y. et al.[47]	https://bioconductor.org/packages/devel/bioc/html/Rsubread.html
EdgeR v.3.34.1	Robinson et al.[48]	https://bioconductor.org/packages/devel/bioc/html/edgeR.html

(*Continued on next page*)

Continued

REAGENT or RESOURCE	SOURCE	IDENTIFIER
ROTS	Suomi T. et al.[49]	https://www.bioconductor.org/packages/release/bioc/html/ROTS.html
Seurat v5	Hao, Y. et al.[50]	https://satijalab.org/seurat/articles/install.html
ScPubr	Blanco-Carmona, E. et al.[51]	https://github.com/enblacar/SCpubr

EXPERIMENTAL MODEL AND STUDY PARTICIPANT DETAILS

Institutional review board statement

Umbilical cord blood was obtained from healthy neonates, both sexes, at Turku University Central Hospital for this study. The usage of the cord blood of unknown donors was approved by the Ethics Committee of Hospital District of Southwest Finland (Dated: 24.11.1998; ethical approval number: 323). As the subjects were neonates, informed consent was obtained from the parents or their legal representatives. Cord blood samples have been collected anonymously without any information on the sex of the neonates.

Human primary T cell isolation, activation, and culture conditions

Total $CD4^+$ T cells were isolated from human umbilical cord blood samples collected from Turku University hospital from full-term normal delivery. Mononuclear cells were isolated using Ficoll density gradient centrifugation. $CD4^+$ cells were then enriched using bead-based positive isolation (Dynal CD4 Positive Isolation Kit; Invitrogen, Cat. no. 11331D). The isolated $CD4^+$ cells were constituted of approximately 90% $CD45RA^+$ $CD45RO^-$ naive T cells (Figure S1). Alternatively (for experiments shown in Figure S2), naïve $CD4^+$ cells were enriched using bead-based negative isolation kit (EasySep™ Human Naïve $CD4^+$ T Cell Isolation Kit; StemCell Technologies, Cat. no. 18000).

Cells were activated using plate-bound α-CD3 (3.75 μg/ml; Beckman Coulter, Cat. no. IM1304) and soluble α-CD28 (1 μg/ml; Beckman Coulter, Cat. no. IM1376) in RPMI 1640 medium (Sigma-Aldrich) supplemented with L-glutamine (2 mM, Sigma-Aldrich), antibiotics (50 U/ml penicillin plus 50 μg/ml streptomycin; Sigma-Aldrich) and 10% FCS. All cultures were maintained at 37°C in a humidified atmosphere of 5% (v/v) CO_2 incubator. For the TGF-β titration experiment, cells were activated for 72 h in the presence of variable TGF-β (R&D systems) concentration.

Controls

For knockdown experiments, cells transfected with non-targeting control LNAs were used as negative controls. Cytokine stimulation experiments included unstimulated cells as baseline controls.

METHOD DETAILS

T cell activation titration, cell viability and proliferation assay

For α-CD3 and α-CD28 activation titration experiment, cells were harvested 24 h post activation with variable α-CD3 and α-CD28 concentrations. The cells were then stained with α-CD69 (BD Pharmigen 347823) and α-CD25 (BD Pharmigen 567316) antibodies and analyzed by flow cytometry. For cell viability assay, cells nucleofected with LNA1, LNA2 or NT (Non-Targeting) were rested for 24 h after which they were activated as mentioned above. We used a fixable cell viability dye (eBioscience™ Fixable Viability Dye eFluor™ 780) to test for cell viability using flow cytometry. Staining was done following manufacturer's instructions.

For cell proliferation assay, cells were nucleofected with LNA1, LNA2 or NT LNAs, rested for 24 h, stained with CellTrace Violet and were activated as mentioned above. The proliferation was checked by flow cytometry after 96 h of activation.

Gene knockdown

LINC01871 was silenced using two LNAs targeting different regions of the gene (LNA1: 5'-TTCGGCCTTTGGTAGT-3'; LNA2: 5'-ACA-GATCGTCCACGGC-3') or non-targeting LNA (NT) (5'-AACACGTCTATACGC-3'). Cells were transfected with LNAs as described before.[10] Briefly, 4 million cells, resuspended in 100 μl OptiMEM medium (Gibco by Life Technologies, Cat. no. 31985-047), were transfected with 300 pmol of LNA using Amaxa nucleofector system (Nucleofector 2C / U-014 program) (Lonza). After nucleofection, cells were rested in RPMI medium, supplemented with pen/strep, 2 mM L-glutamine and 10% FCS, for 24 h at 37°C followed by their activation, as described above.

Cellular fractionation

The fractionation was performed with 20 million cells. First, the cell membrane was lysed with hypotonic lysis buffer (10 mM HEPES, 10 mM KCl, 1.5 mM $MgCl_2$, 0.34 M sucrose, 10 % glycerol; pH 7.5) supplemented with 1 mM DTT and complete Protease Inhibitor Cocktail (Roche). After incubating the cells with the buffer on ice for 10 min, 0.5% Triton X-100 was added to complete the cell lysis,

and the cells were further incubated for 10 min on ice. The nuclei were collected by centrifugation (1300 x g, 4 °C, 5 min), and the supernatant containing the cytoplasmic fraction was separated. The nuclei were washed with cold hypotonic lysis buffer (centrifugation 1300 x g, 4 °C, 5 min), and the supernatant was discarded. The nuclei were then lysed with cold nuclear lysis buffer (incubation 30 min on ice), and the chromatin was collected by centrifugation (1700 x g, 4 °C, 10 min). The supernatant containing the nucleoplasm fraction was collected, and the pellet containing the chromatin was washed with nuclear lysis buffer. RNA was isolated from each fraction with RNeasy Mini Kit (Qiagen). The fractionation was confirmed by running qRT-PCR with known cell compartment-specific RNAs.

RNA isolation and TaqMan qRT-PCR assay

RNA was isolated using the RNeasy Mini Kit (QIAGEN). The removal of genomic DNA was done in-column with DNase treatment (RNase-Free DNase Set; QIAGEN) for 15 min, followed by an additional treatment of the samples with DNase I (Invitrogen). Nanodrop 2000 (ThermoFisher Scientific) and Experion Automated Electrophoresis System (BioRad) were used to measure the quantity and quality of RNA, respectively. SuperScript II Reverse Transcriptase (Invitrogen, Cat. no. 18064-014 and 18418012) was used for cDNA synthesis, according to the manufacturer's instructions. TaqMan qRT-PCR reactions were run on QuantStudio™ 12K Flex Real-Time PCR System (Thermo Fisher Scientific), and the data were analyzed using Quantstudio software (Thermo Fisher Scientific). All TaqMan reactions were performed using Absolute QPCR Mix, ROX (Thermo Scientific, Cat. no. AB1139A). The cycle threshold (CT) values of the samples were normalized to the CT values of the endogenous control housekeeping gene eEF1A,[52] generating delta CT (dCT) values. The following TaqMan primers and probes were used: LINC01871 (forward: 5'-agcatgcagcaactacagtca-3'; reverse: 5'-cagcttcggcctttggta-3', and probe #78 from Roche Universal Probe Library (UPL); EF1-α (forward primer: 5'-ctgaaccatccaggccaaat-3', reverse primer: 5'-gccgtgtggcaatccaat-3', and Probe FAM-TAMRA: 5'-agcgccggctatgcccctg-3'); MALAT1 (forward primer: 5'-gacccttcacccctcacc-3', reverse primer: 5'-ttatggatcatgcccacaag-3' and probe #71 from UPL); IL2RA (forward primer: 5'-acgggaagacaaggtggac-3', reverse primer: 5'-tgcctgaggcttctcttca-3', and Probe #54 from Universal Probe Library). The CD69 TaqMan assay was from ThermoFisher: (assay ID: Hs00934033_m1).

RNA-seq analysis

Libraries for RNA-Seq were prepared at the Finnish Functional Genomics Centre, using Illumina TruSeq Stranded mRNA Sample Preparation Guide (part # 15031047). The quality of the libraries was confirmed with Advanced Analytical Fragment Analyzer, and the concentrations of the libraries were quantified with Qubit® Fluorometric Quantitation (Life Technologies). Nine samples were pooled and sequenced on one lane of NovaSeq 6000 SP flow cell v1.5 Next-Generation Sequencing platform with 2x150bp read length. Sequencing was performed at the Finnish Functional Genomics Centre. FastQC (v.0.11.8)[46] was used to check the quality of the raw sequencing reads. Rsubread (v.2.6.4)[47] was used to align the reads to the human reference genome hg38 and count the read for each RefSeq gene. The data was normalized as CPM (counts per million) values using EdgeR (v.3.34.1).[48] Log2 transformed normalized data was used for differential expression analysis using the tool ROTS,[49] as genes with the false discovery rate (FDR) $\leq$ 0.05.

Mass spectrometry (MS)

The cell pellet was lysed in a lysis buffer (4% SDS in 50 mM TRIS-HCl, pH 7.6) followed by Benzonase treatment for 10 minutes at room temperature. The extract was then clarified by centrifugation at 13,000 x g for 10 minutes. Protein concentration was determined using a DC assay. Subsequently, dithiothreitol (DTT) was added to a final concentration of 10 mM, followed by addition of iodoacetamide (IAA) to a final concentration of 20 mM. After incubation for 30 minin the dark, the lysate was digested using the Suspension Trapping (STrap) method as described previously.[53] The dried peptides were reconstituted in a formic acid/acetonitrile mixture, and 800 ng of peptide mixture was analyzed using an EasynLC 1200 coupled to an Orbitrap Fusion™ Lumos™ mass spectrometer (Thermo Scientific). Protein identification and quantification was performed as described earlier.[10]

Overall, the proportion of missing (zero) values in the data was very low (0.22%). The MS2-level quantity data were obtained, and proteins quantified with only one peptide across the entire experiment were filtered out as unreliable. Subsequently, the data was offset with +1 and $\log_2$-transformed. The DE proteins between the LINC01871-silenced and control T cells were identified using ROTS,[49] as proteins with FDR $\leq$ 0.05.

Mass cytometry

After activation, cells were stained with Cell-ID Cisplatin to identify viable cells as recommended by the manufacturer (Standard Biotools, USA). Next, cells were stained with metal-conjugated phosphoprotein antibodies (anti-pS6 -175Lu, [S235/S236], clone N7-548; anti-pPLCg2 – 144Nd [Y759], clone K86-689.37; anti-pERK1/2 – 167Er [T202/Y204], clone D1314.4E; anti-pSLP-76 – 156Gd [Y128], clone J141-668.36.58; anti-pZAP70 - 171Yb [Y319]/pSyk [Y352], clone 17a; anti-pLck – 162Dy [T505], clone 4/LCK-Y505; anti-pAkt – 152Sm [S473], clone D9E; anti-pStat5 – 150Nd [Y694], clone 47) according to the manufacturer's protocol "Maxpar phosphoprotein staining with fresh fix" (Standard Biotools, USA). Finally, the cells were incubated with Cell-ID intercalator solution (Standard Biotools, USA) at concentration of 125 nM overnight at 4°C. For the analysis, cells were diluted to $0.5x10^6$ cells/ml with cell acquisition solution (Standard Biotools USA) and analysed on Helios mass cytometer (Standard Biotools, USA). Data were analyzed using FCS Express 7 Flow software v. 7 (*De Novo* Software, USA).

ELISA

Secreted IL-2 levels were estimated (Human IL-2 DuoSet ELISA, R&D Systems, Cat. nos. DY202-05, DY008) using cell culture supernatants of T cells activated for 48 h. The amount of IL-2 was normalized with the number of living cells determined by forward and side scattering in flow cytometry analysis (LSRII flow cytometer; BD Biosciences).

RACE-PCR and sanger sequencing

Using the SMARTer RACE cDNA Amplification Kit (Takara Bio/Clontech, Cat. nos. 634858, 634859), 5'and 3'cDNA templates were prepared from total RNA, isolated from T cells activated for 48 h, according to the kit protocol. Amplification of 5'and 3'cDNA ends was done using gene-specific primers (5'-RACE: 5'-gcatgctgaacccaggcagctgactccagag-3'; 3'-RACE: 5'-ctctggagtcagctgcctgggtt cagcatgc-3') and the kit-supplied universal primer. Products from these PCR reactions were diluted and used as templates for running nested PCR with nested gene-specific primers (5'-RACEnested: 5'-ctctgttgctcagcttcggcctttgg-3; 3'-RACEnested: 5'-gctgc cgtggacgatctgtctctc-3') and nested universal primer. The RACE-PCR products were analyzed by agarose gel electrophoresis, and PCR products were cut out from gel. The DNA was extracted using GeneJet Gel Extraction Kit (Thermo Scientific, Cat. no. K0692), quantified with NanoDrop 2000, and analyzed by Sanger sequencing at the Institute for Molecular Medicine *Finland (FIMM), University of Helsinki.*

Reanalysis of published scRNA-seq datasets

Seven of the single cell datasets were downloaded from CellxGene (https://cellxgene.cziscience.com/) and two from the Single Cell Portal (https://singlecell.broadinstitute.org/single_cell). See Table S1 for an origin of the datasets. All analysis and visualization were performed with Seurat v5[50] and ScPubr[51] in R. In order to homogenize and compare cell types across the different datasets, reference annotation with Azimuth was applied using the bone marrow reference. Differential expression analysis was carried out with ''FindMarkers'' from Seurat v5. Mean gene Pearson correlation was calculated in R, using the corr.test function.

QUANTIFICATION AND STATISTICAL ANALYSIS

The data were plotted using Prism version 9. Whenever applicable, the error bars represent SD. For comparing the means of multiple samples, the statistical significance of the differences between means were determined by one-way ANOVA followed by Šídák's multiple comparisons test or test for linear trend analysis. For comparing the means of two samples, the significance was determined using unpaired two-tailed t-test. $p < 0.05$ was considered significant.